International Journal of Biological Macromolecules 51 (2012) 879–886

Contents lists available at SciVerse ScienceDirect

International Journal of Biological Macromolecules

journal homepage: www.elsevier.com/locate/ijbiomac

An amperometric glutathione biosensor based on chitosan–iron coated gold nanoparticles modified Pt electrode

Nidhi Chauhan, Jagriti Narang, Meena, C.S. Pundir*

Department of Biochemistry, M. D. University, Rohtak 124 001, Haryana, India

ARTICLE INFO

Article history:
Received 27 July 2012
Accepted 8 August 2012
Available online 14 August 2012

Keywords:
Glutathione
Glutathione oxidase
Gold coated magnetic nanoparticles
Chitosan
Amperometric biosensor

ABSTRACT

A method is described for development of an amperometric biosensor for determination of glutathione (GSH), by immobilizing covalently a glutathione oxidase (GSHOx) onto the surface of gold coated magnetic nanoparticles (Fe@AuNPs) modified Pt electrode. Chitosan was used to introduce amino groups onto the surface of Fe@AuNPs. The morphology and covalent linkage of GSHOx led to high enzyme loading and better shelf life. The enzyme electrode was characterized by scanning electron microscopy (SEM), cyclic voltammetry (CV), Fourier transform infrared (FTIR) and electrochemical impedance spectroscopy (EIS). The electrode showed maximum response within 4 s, when polarized at +0.4 V, pH 7.0 and 25 °C. There was a linear relationship between electrode response and glutathione concentrations in the range 5.0–4000 μmol L^{-1} with a detection limit of 0.1 μmol L^{-1}. An amperometric method of GSH determination was developed using this biosensor. The evaluation studies showed that the method was reliable as mean analytic recoveries of 50 μM and 100 μM of GSH were 97.5 ± 1.7 and 96.1 ± 1.3 respectively and within and between CVs for glutathione determination in blood RBCs were <2.14% and <2.39% respectively. The biosensor showed 50% loss in its initial activity after its 150 uses over a period 4 months, when stored at 4 °C. GSH concentration in hemolysated erythrocytes as measured by the present biosensor was 2.8 mmol L^{-1} in apparently healthy persons.

1. Introduction

Glutathione (GSH) a tripeptide, is widely distributed in the living systems and involved in many crucial processes in the cells. It plays an important role in the metabolism of many drugs and endogenous substances and maintains the integrity of erythrocytes [1]. It is the essential component of antioxidant defense systems, which plays an important role in cellular protection against injuries [2]. This GSH protective mechanism results in an increased formation of glutathione disulphide compound (GSSG) [3]. Normally, the ratio of GSH to GSSG is used as an indicator of oxidative stress and of great importance in pathology and clinical application [4]. Therefore, it is necessary to approach for a reliable and durable measurement of GSH and GSSG to facilitate the determination of GSH to GSSG ratio and the subsequent investigation of oxidative stress and the toxicity mechanism. The ratio has gained much attention in recent years, due to its vital biological functions such as involvement in bioreductive reactions, enzyme activity maintenance, amino acid transport, protection against oxidative stress and detoxification [5]. There is also a direct correlation between the quantity of reduced GSH in intracellular fluids and aging of life [6]. GSH is over expressed in many tumor tissues and altered levels of GSH in plasma have been implicated in diagnosis of a number of pathological conditions, including Alzheimer's, Parkinson's diseases, diabetes, macular degeneration and HIV disease [7,8]. Hence, detection of GSH in blood RBCs is very important. Therefore, more and more sensitive analytical methods for determination of GSH are highly demanded. Some analytical methods combined with different detection techniques have been developed for the analysis of GSH. Since GSH do not have spectroscopically active groups, detection systems based on fluorimetric [9], colorimetric micro-method [10], enzymatic recycling method [11], chemiluminescence method [12], reverse-phase HPLC method [13], spectrofluorimetric method [14], iodine method [15] and HPLC analysis [16] need derivatization, which is time consuming and involves the risk of oxidation of GSH. Nevertheless, simplicity, rapidity, high sensitivity, specificity and low cost are the main advantages of biosensing techniques for the analysis of biological compounds [17]. Modern biosensors based on nanoscale techniques have the potential to improve the methods of GSH detection and may result in cheaper, faster and easier-to-use analytical tools. Furthermore, nanoscale biosensors may be more portable and scalable for point-of-care sample analysis and real-time diagnosis. Several electrochemical detection methods, mostly

* Corresponding author. Tel.: +91 9416492413; fax: +91 1262 294640.
E-mail addresses: pundircs@rediffmail.com, pundircs@gmail.com, pundircs@yahoo.com (C.S. Pundir).

0141-8130/$ – see front matter © 2012 Elsevier B.V. All rights reserved.
http://dx.doi.org/10.1016/j.ijbiomac.2012.08.008

based on oxidation of GSH on unmodified [15,18] or chemically modified electrodes have been reported [7,19–21].

However, all these biosensor had some common drawbacks such as low sensitivity, low storage stability and reusability. Recently, nanomaterials have been employed for the improved performance of electrochemical biosensors [22–26]. Magnetic nanoparticles (Fe_3O_4NPs) owe their popularity to their numerous attributes such as their magnetic properties that enable them to be directed by an external magnetic field, the possibility to separate them from a reaction mixture, in addition to their low toxicity and biocompatibility. Unfortunately, Fe_3O_4NPs with a large surface area are easily oxidized, i.e. they react vigorously with oxygen present in the air and also react between themselves forming aggregates. To overcome this problem, the surface of NPs has been coated. Among the various materials used for coating [27,28], gold has become a favored coating material, because of its simple synthetic procedure and chemical functionality [29]. It is expected that Fe_3O_4NPs can avoid being oxidized and maintain their magnetic properties (such as coercivity or blocking temperature) by the gold coating. Thus, the magnetic cores could be protected from oxidation and corrosion [30–32].

Meanwhile, chitosan (CHIT) has become a widespread biopolymer owing to its remarkable chemical and biological characteristics. It is a hydrophilic material due to the presence of both amino and hydroxyl groups; however, CHIT is insoluble in water and aqueous basic media [33]. It was chosen as the orientation directing matrix because there are large quantities of amino and hydroxyl groups on the CHIT units, which have a strong binding ability to enzyme [33–38].

To the best of our knowledge, no attempt has been made to employ Fe@Au nanomaterials for the improvement of GSH biosensor. In the present report, we describe for the first time, the construction of an amperometric GSH biosensor based on covalent immobilization of glutathione oxidase (GSHOx) onto CHIT/Fe@Au/Pt electrode. The use of covalently immobilized GSHOx onto these Fe@AuNPs is expected to improve the analytic performance of GSH biosensor.

2. Materials and methods

2.1. Chemicals and reagents

Glutaraldehyde (grade 1, 25%) from Sigma Chemical Co St. Louis, USA, $FeCl_2{\cdot}4H_2O$ and $FeCl_3{\cdot}6H_2O$, $HAuCl_4$ (~49% Au), sodium citrate ($Na_3C_6H_5O_7$) (extra pure AR), NaOH (97%), tetramethylammonium hydroxide (TMOH) (25%, aquous solution pure), glutathione oxidase, glutathione and chitosan (MW ~ 1 × 106; 75–85% deacetylation) from Sisco Research Laboratory, Mumbai, India were used. HCl (35.4%) and HNO_3 (69–70%) from LOBA CHEMIE PVT. LTD., Mumbai, India were used. Pt wire (1.5 cm × 0.05 cm) was purchased from local market. All other chemicals were of analytical reagent (AR) grade. Double distilled water (DW) was used throughout the experiments.

2.2. Apparatus

All electrochemical experiments, including cyclic voltammetry (CV) and electrochemical impedance spectroscopy (EIS) measurements were carried out in a Potentiostat/Galvanostat (Autolab, Eco Chemie, The Netherland. Model: AUT83785 with General Purpose Electrochemical System (GPES), software, version 4.9) with a three electrode system consisting of a Pt wire as an auxiliary electrode, an Ag/AgCl (3 M KCl) electrode as reference electrode and modified Pt wire as a working electrode. Fourier Transform Infrared (FTIR) spectroscopy was carried out in FTIR spectrometer (mode iS10, Thermoelectron, USA) and scanning electron microscopy (SEM) of bare Pt and GSHOx/Fe@Au modified Pt electrode were carried out at AIRF, J.N.U., New Delhi on commercial basis to confirm immobilization of GSHOx. To determine the size of Fe@Au NPs, an aqueous solution of Fe@Au powder (1 mg mL^{-1}) was subjected to transmission electron microscopy (TEM) at Punjab University, Chandigarh. X-ray diffraction (XRD) studies of Fe@Au NPs were carried out at Physics Department G. J. University, Hisar, using X-ray diffractometer (Make: Rigaku Mini Flex II, Americas Corporation).

2.3. Synthesis of Fe_3O_4NPs

The Fe_3O_4NPs (cores) were prepared by co-precipitation of Fe(II) and Fe(III) chlorides (FeII/FeIII ratio of 0.5) in an alkaline solution by the method of Kang et al. with some modifications [39]. Briefly, 4.595 g of Fe(III) chloride and 1.71 g of Fe(II) chloride were dissolved in 20 mL of DW in the presence of 100 mL of 2 M HCl. The solution was then stirred vigorously until the Fe salt was dissolved. Subsequently, a solution of 2 mol L^{-1} NaOH was added dropwise into this solution under vigorous stirring, resulting in a pale yellow coloured solution, which was changed to brown and finally dark black coloured solution. The black precipitates were collected on a magnet and washed twice with DW and once with 0.1 mol L^{-1} TMOH and then isolated by centrifugation. To obtain oxidized Fe_3O_4NPs, the precipitates (from above) were first washed in 0.01 mol L^{-1} HNO_3, the particles were then suspended in 0.01 mol L^{-1} HNO_3 and finally heated at 80–90 °C under constant stirring, until the appearance of brown colour [40]. The oxidized Fe_3O_4NPs were suspended in 0.1 mol L^{-1} TMOH at pH 11 after washing with DW.

2.4. Preparation of Au–Fe oxide composite nanoparticles (Fe@Au)

Au-shell coating was carried out by reduction of Au^{3+} on the surface of Fe oxide according to Brown and Natan's boiling citrate seeding procedure with modification [41]. One milliliter of the above prepared 0.212 mmol L^{-1} tetra methyl amine-stabilized oxidized Fe_3O_4 stock solution was diluted with 50 mL of 0.01 mol L^{-1} sodium citrate and stirred for 30 min to exchange absorbed OH^- with citrate ions to make the final working magnetic-core solution. The oxidized Fe_3O_4NPs (0.1 mg mL^{-1}) from the working magnetic-core solution were used for the Au coating reaction in a total volume of 40 mL of 0.01 mol L^{-1} sodium citrate. The reaction solution containing magnetic cores and reduction agent was first sonicated for 15 min and then heated to boiling with vigorous stirring. Solution of 10 nmol L^{-1} $HAuCl_4$ was added as soon as the reaction solution reached the boiling point. Fifteen minutes after addition of Au^{3+} salts, the heating was stopped and the stirring was continued till, the solution was cooled to room temperature [42].

2.5. Preparation of CHIT/Fe@Au modified Pt electrode

Prior to the surface modification, the Pt electrode was cleaned with piranha solution [H_2SO_4:H_2O_2 in ratio 3:1 (v/v)] for 20 min (CARE) and then rinsed thoroughly with DW. Then the electrode was polished with alumina slurry. Fe@Au NPs were electrochemically deposited onto Pt electrode through cyclic voltammetry (CV) technique by immersing cleaned Pt electrode in a solution (25 mL) containing 22 mL electrolyte [2.5 mM $K_3Fe(CN)_6$/$K_4Fe(CN)_6$ (1:1)] and 3 mL bionanoparticles (in 0.1 mol L^{-1} KCl) and then applying 20 polymerization cycles at −0.6 to +0.6 V at a scan rate of 50 mV s^{-1}. The resulting Fe@Au/Pt modified electrode was washed thoroughly with DW to remove unbound matter and kept in dry petri plate at 4 °C. The Fe@Au modified Pt electrode was dipped into 5% chitosan (in 2% acetic acid) solution and the kept for 12 h at 4 °C [22].

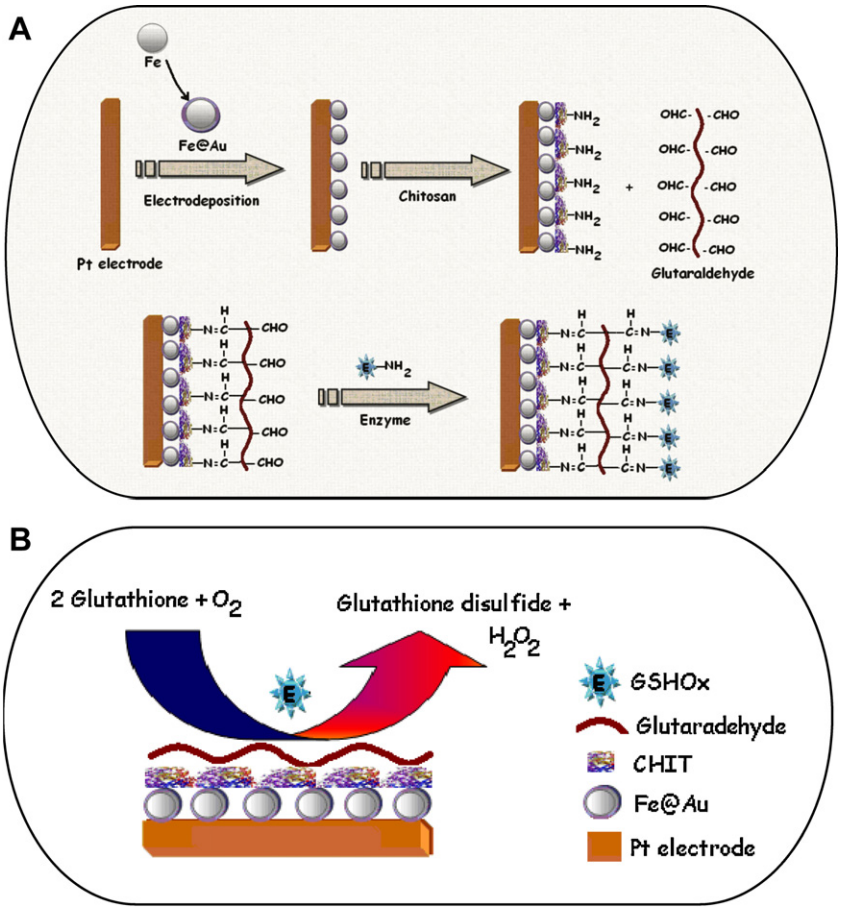

Scheme 1. (A) Schematic of the modification of Pt electrode with CHIT/Fe@Au nanoparticles and GSHOx for efficient detection of glutathione (B) The mechanism of glutathione measurement by GSHOx/CHIT/Fe@Au modified Pt electrode.

2.6. Preparation of enzyme electrode (GSHOx/CHIT/Fe@Au/Pt electrode)

GSHOx was immobilized covalently onto the CHIT/Fe@Au modified Pt electrode surface after glutaraldehyde cross-linking. The GSHOx enzyme electrode was constructed by activating CHIT/Fe@Au modified Pt electrode with 1.0 mL of 2.5% glutaraldehyde for 2 h at room temperature followed by thorough washing with DW and then immobilizing 100 μL GSHOx solution (1 mg mL^{-1}) onto this glutaraldehyde activated Pt electrode surface. The resulting enzyme electrode was washed thoroughly with DW, dried and then stored in the refrigerator at 4 °C.

2.7. Scanning electron microscopy (SEM)

SEM images of bare Pt, Fe@Au/Pt and GSHOx/CHIT/Fe@Au/Pt electrodes were taken out to study immobilization of GSHOx. The electrodes were cut in small pieces (1 cm × 1 cm) and placed on copper mount of 2 cm diameter. The gold particles were deposited on its surface using spray gun and their micrographs were taken in a scanning electron microscope.

2.8. Construction and response measurement of GSH biosensor

A method is described for construction of an amperometric GSH biosensor by connecting GSHOx/CHIT/Fe@Au/Pt electrode as working electrode, Ag/AgCl (3 M KCl) as reference electrode and Pt wire as auxiliary electrode. To test the functioning of the biosensor, three electrodes immersed into 15 mL 0.05 mol L^{-1} sodium phosphate (pH 6.5) in a 50 mL beaker. The reaction was started by adding GSH solution (1 μmol L^{-1}) to reach a final concentration of 100 μM and the current (mA) generated was recorded from 0.0 to +0.6 V vs. Ag/AgCl (3 M KCl) as reference. The maximum response i.e. current was observed at +0.4 V and hence subsequent studies were carried out at this potential.

2.9. Optimization of GSH biosensor

The effect of pH of the buffer was studied over the pH range 5.0–8.0 at interval of 0.5, using 0.1 M sodium phosphate buffer (6.0–8.0) and acetate buffer (5.0–5.5). The effect of temperature on GSHOx/CHIT/Fe@Au/Pt electrode was studied by incubating the reaction mixture at different temperature (20–50 °C at an interval of 5 °C). The effect of response time on GSHOx/CHIT/Fe@Au/Pt electrode was studied at different time (2–12 s at an interval of 2 s). The effect of GSH concentration on biosensor response was determined by varying the concentration of GSH in 15 mL reaction mixture ranging from 5.0 to 4000 μM. The detection limit (LOD) of the present biosensor was calculated as the lowest quantity of GSH required to give a signal to a background (blank) +3 times SD of blank. The amperometric response was also measured in presence of possible interfering compounds and metabolites such as methionine, cysteine, glutamic acid, glycine, ascorbic acid, uric acid and EDTA at a final concentration of 0.1 mmol L^{-1}.

2.10. Collection of venous blood and analysis of GSH content in human erythrocyte

The GSH content in human erythrocytes was measured with the present biosensor as follows. Venous blood was collected from Hospital of Pt. BDS University of Health & Medical Science, Rohtak and stored at −20 °C until use. In venous blood, solid EDTA, 1 mg mL^{-1} (final concentration in solution), was added as anticoagulant. The blood was centrifuged at 3000 rpm for 15 min. Packed erythrocytes were then collected, washed with a saline isotonic solution (0.9% NaCl) and stored at 4 °C until use. The erythrocytes were hemolysated in 5 mmol L^{-1} of EDTA solution and diluted in 1:l00 ratio with the working buffer for analysis. All experiments were carried out at 25 °C. The amperometric determination of GSH was carried out in same manner as described earlier for response measurement of biosensor under optimal conditions except that GSH was replaced by hemolysated erythrocytes. The concentration of glutathione was interpolated from calibration curve between current (mA) vs. GSH concentration.

3. Results and discussion

The fabrication of a GSHOx electrode based on covalent immobilization of GSHOx onto Fe@Au modified Pt electrode is summarized in Scheme 1A. Firstly, Fe@AuNPs was deposited electrochemically on the surface of Pt electrode, as this method is easy and the layer thickness could be controlled. Our results showed that Fe@AuNPs provided a remarkable synergistic effect towards the oxidation of GSH. Enzyme was immobilized covalently by formation of covalent bond (C=N bond) between —NH_2 groups on surface of enzyme and —CHO group of glutaraldehyde.

3.1. Nanoparticles characterization

The crystallographic analysis of the samples was performed by powder X-ray diffraction (XRD). Diffraction patterns (vs. 2θ) were recorded with an X-ray diffractometer (Fig. 1A). The pattern shows the presence of both Fe and Au with some peaks overlapping, consistent with the previous reports [29,43]. Notably, no iron oxide's peak was found in Fig. 1A and also no oxygen was detected in XRD measurements. This indicates clearly that the iron core was protected by the gold shell from oxidation. Fig. 1B shows typical morphologies of the synthesized nanoparicles and their aggregates. Since the Fe_3O_4NPs are magnetic at room temperature, they tend to aggregate on the grid. The core–shell structure of the nanoparticles is evident in Fig. 1B. This core–shell structure means that the formation of Au layers on the surface of the pre-existing FeNPs was preferred to the homogeneous nucleation of pure AuNPs. Fe@AuNPs synthesized in this study was essentially very fine and monodisperse with diameter of ca. 30–60 nm as seen from TEM image (Fig. 1B).

3.2. Evidence of enzyme immobilization

The morphology of bare Pt electrode, CHIT/Fe@Au/Pt electrode and GSHOx/CHIT/Fe@Au/Pt electrode was characterized by SEM studies. SEM of the bare Pt electrode (Fig. 2A) showed a smooth and featureless morphology, however, the tubular structures and granular structures in Fig. 2B account for the presence of Fe@Au and CHIT on the surface of Pt electrode. Globular shapes on the electrode surfaces (Fig. 2C) display presence of GSHOx layer after immobilization.

The FTIR spectra of CHIT/Fe@Au/Pt and GSHOx/CHIT/Fe@Au/Pt electrodes are given in Fig. 3A. The CHIT exhibited characteristic absorption bands of amino saccharide at 3421 cm^{-1} (due to overlapping of —OH and —NH_2 stretching), 2811 cm^{-1} (due to–CH_2

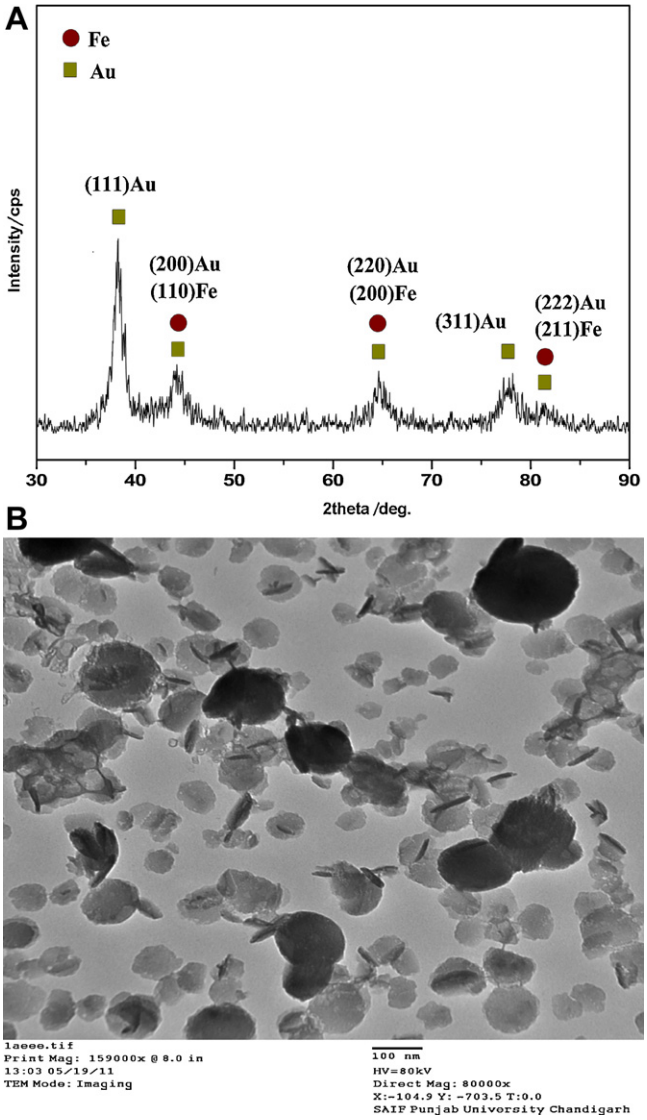

Fig. 1. (A) The X-ray diffraction pattern of iron oxide nanoparticles and (B) transmission electron microscopy image of Fe@Au.

stretching) and 1647 cm^{-1} (due to C–O stretching), while the CHIT/Fe@Au composite film showed additional peak at 492 cm^{-1} corresponding to the Fe@AuNPs (curve i). The enzyme mixture was immobilized onto chitosan through covalent binding with glutaraldehyde. One —CHO group of glutaraldehyde was linked to —NH_2 group on surface of enzymes, while other —CHO group was bound to —NH_2 group of chitosan on CHIT/Fe@Au composite film, which provided physically more stable complex. FTIR spectra of GSHOx/CHIT/Fe@Au/Pt electrode showed broadening of the peak at 3264 cm^{-1} and 1653 cm^{-1} due to the addition of carbonyl and amino groups confirming the binding of enzyme with the CHIT/Fe@Au matrix (curve ii).

Fig. 3B shows electrochemical impedance spectra (EIS) of (a) Fe@Au/Pt electrode (b) CHIT/Fe@Au/Pt electrode and (c) GSHOx/CHIT/Fe@Au/Pt bioelectrode. The charge transfer process in GSHOx/CHIT/Fe@Au/Pt bioelectrode has been studied by monitoring charge transfer resistance (R_{CT}) at the electrode and electrolyte interface. The value of the electron transfer resistance (semicircle diameter) (R_{CT}) depends on the dielectric and insulating features at the electrode/electrolyte interface. The R_{CT} values for the Fe@Au/Pt electrode, CHIT/Fe@Au/Pt electrode and GSHOx/CHIT/Fe@Au/Pt bioelectrode have been obtained as 5.7×10^2, 4.2×10^2 and

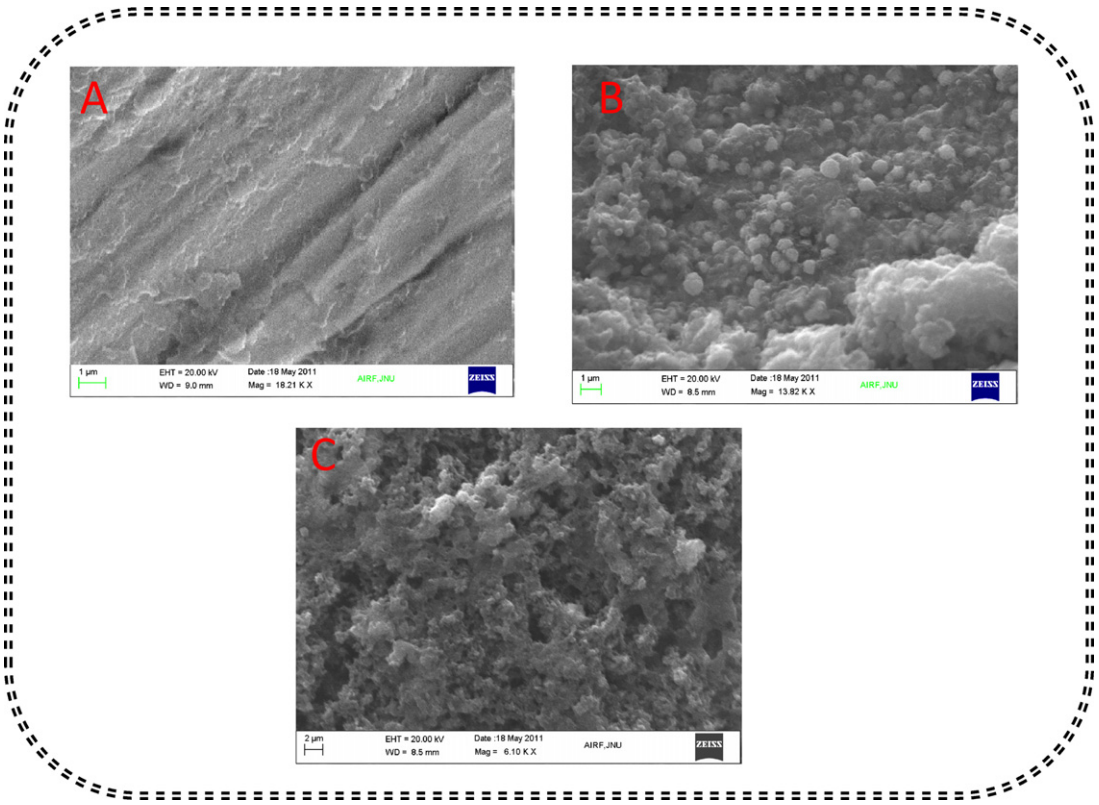

Fig. 2. (A) SEM of bare Pt electrode, (B) CHIT/Fe@Au modified Pt electrode and (C) GSHOx/CHIT/Fe@Au/Pt electrode.

$9.5 \times 10^2\ \Omega$ respectively. The electron transfer via redox couple is hindered by the presence of enzymes on electrode surface. The increased R_{CT} value of GSHOx/CHIT/Fe@Au/Pt electrode was due to the immobilization of enzymes onto GSHOx-CHIT/F@Au/Pt surface. This increase in R_{CT} is attributed to the fact that most biological molecules, including enzymes, are poor electrical conductors at low frequencies (at least <10 kHz) and cause hindrance to the electron transfer.

3.3. Response towards GSH at the GSHOx/CHIT/Fe@Au/Pt electrode

In order to evaluate the charge-transfer properties on the surface of the modified electrodes, cyclic voltammetry technique was employed, using $K_3Fe(CN)_6/K_4Fe(CN)_6$ as redox probe. Cyclic voltamogramms recorded in 10 mmol L^{-1} $K_3Fe(CN)_6/K_4Fe(CN)_6$ solution and sodium phosphate buffer 0.1 mol L^{-1} (pH 7.0) are shown in Fig. 4A. For bare Pt electrode, the well defined oxidation and reduction peaks caused by Fe^{3+}/Fe^{2+} redox couples were noticed in forward and reverse scan [Curve (a)]. After the electrode was modified by F@AuNPs current response of CVs was increased [Curve (b)]. The values of the peak separation (difference between anodic peak potential and cathodic peak potential, Δ Ep) were also determined. The obtained values on bare Pt electrode and F@AuNPs modified Pt electrode were +290 mV and +440 mV respectively. The electrodeposition of F@AuNPs on Pt electrode surface led to vast increase in current intensity as a result of the increase in electro active area. The preservation of a quasi reversible electrode process and the large increase in peak currents for the nanocomposite film modified electrode proved that F@AuNPs exerted an obvious improvement effect on electric conductivity of enzyme electrode.

To evaluate the catalytic activity of GSHOx at the GSHOx/CHIT/Fe@Au modified Pt electrode, the modified electrode was characterized by a cyclic voltammogram in the presence of GSH in the potential range from 0.0 V to +0.6 V. Fig. 4B shows cyclic voltammograms of the GSHOx/CHIT/Fe@Au modified Pt electrode in an unstirred 0.1 M KCl solution and 0.1 mol L^{-1} acetate buffer (pH 5.5) with (curve b) and without GSH solution (curve a) at scan rate 50 mV s^{-1}. It was observed that with the addition of 1.0 mmol L^{-1} GSH, both the reduction current and oxidation current increased, which showed the improved catalytic properties of modified electrode to the oxidation of GSH (Scheme 1B).

3.4. Optimization of biosensor

The effect of pH from 5.0 to 8.0 for 50 μmol L^{-1} GSH solutions was investigated. The current response resulting from the CHIT/Fe@Au modified Pt electrode bound enzyme-catalyzed reaction achieved a maximum value at pH 7.0, which is higher than that for silver nanoparticles/MWCNT/polyaniline film (6.0) [44], clark-type oxygen electrode (6.5) [45] but lower than that of pyrolytic graphite electrode (7.8) [46]. This shift in optimum pH from earlier reported biosensor could be related to the functional groups ($-NH_2$) of the polymer side chain. The optimal pH and incubation temperature of biosensor/immobilized GSHOx were 7.0 and 25 °C respectively. The decrease in the optimum temperature compared to free enzyme (30 °C) might be due to the improvement in the enzyme rigidity upon immobilization through covalent binding. The biosensor showed optimum response within 4 s, which is better than earlier reports [44–46].

Fig. 5A showed the cyclic voltammogram of GSHOx/CHIT/Fe@Au modified Pt electrode response at different GSH concentrations (5.0–4000 μmol L^{-1}). There was a linear increase in oxidation current with increase in GSH concentration in the range 5.0–4000 μmol L^{-1} after which, it was constant.

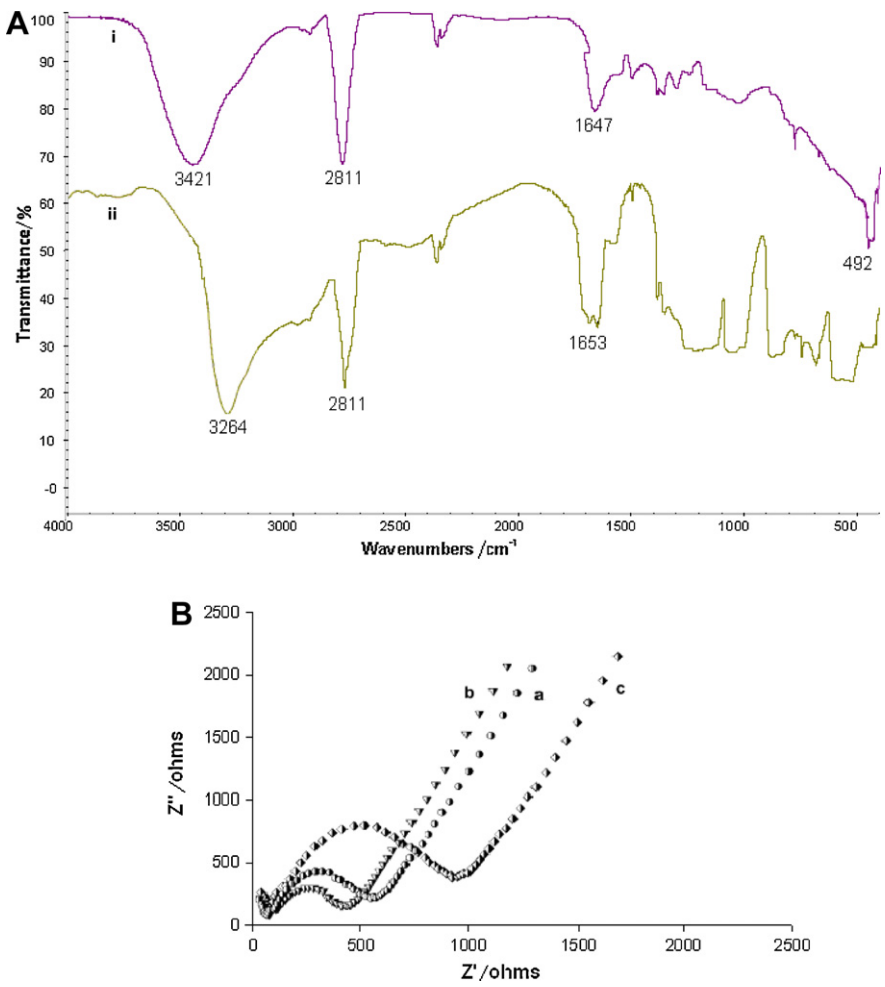

Fig. 3. (A) FTIR spectra of (i) CHIT/Fe@Au/Pt electrode and (ii) GSHOx/CHIT/Fe@Au/Pt electrode.
(B) Nyquist plots of the sensing electrode response at different stages in the electrode assembly process: Fe@Au/Pt (a); CHIT/Fe@Au/Pt (b) and GSHOx/CHIT/Fe@Au/Pt electrode (c). All spectra were recorded in the presence of 10 mmol L^{-1} $[Fe(CN)_6]^{3-/4-}$ in 0.1 mol L^{-1} KCl as a redox-active indicator. Frequency range: 0.01 Hz to 10 kiloHz.

3.5. Evaluation of biosensor

There was a linear relationship between current (mA) and GSH concentration ranging from 5.0–4000 μmol L^{-1} in reaction mixture with a sensitivity of 0.48 mA/μmol L^{-1} (Fig. 5B), which is better than earlier reports (5–10 mmol L^{-1}) [44,45]. The minimum detection limit of the present method was 0.1 μmol L^{-1}. The limit of quantification (LOQ) of the method was 0.303 μmol L^{-1}. The analytic recovery of known amount of added GSH into hemolysated erythrocytes was determined by the present biosensor. The mean analytic recoveries of added 50 and 100 μmol L^{-1} GSH (final conc. in reaction mixture) were 97.5 ± 1.7 and 96.1 ± 1.3 respectively (Table 1), which is comparable to earlier reports 93% and 105% [44]. To test the reproducibility and reliability of the present GSH biosensor GSH content in six hemolysated erythrocytes samples was estimated on single day (within batch) and five times again after storage at −20 °C for one week (between batch). The results showed that determinations were consistent and within and between coefficients of variation (CVs) were 2.14% and 2.39% respectively (Table 2). The high precision indicated the reproducibility and consistency of the present method. Practically no interference (a decrease of only 7.23% for methionine, 5.0% for cysteine, 6.4% for glutamic acid, 9.2% for EDTA, 12.5% for ascorbic acid, 7.5% for uric acid and 5.6% for glycine) was observed during measurements of GSH by the present biosensor response in presence of interference, which is comparable with earlier reports [44,45,47]. The decrease in the current in the presence of interferents may be due to the ionization of the interferent at high voltage, which might cause interference.

A comparison of performance characteristics of the present biosensor with earlier amperometric GSH sensors is summarized in Table 3.

Table 1
Analytical recovery of added glutathione in the hemolysated erythrocytes samples, as measured by GSHOx/CHIT/Fe@Au modified Pt electrode.

Glutathione (μM)	GSH found (μM)	% Recovery
–	30	–
50	78	97.5 ± 1.7
100	125	96.1 ± 1.3

Table 2
Within and between assay coefficients of variation (CVs) for determination of urinary glutathione in the hemolysated erythrocytes samples, measured by GSHOx/CHIT/Fe@Au modified Pt electrode.

n	GSH (μM) Mean ± SD	CVs (%)
Within assay (5)	102.85 ± 2.21	2.14
Between assay (5)	102.47 ± 2.45	2.39

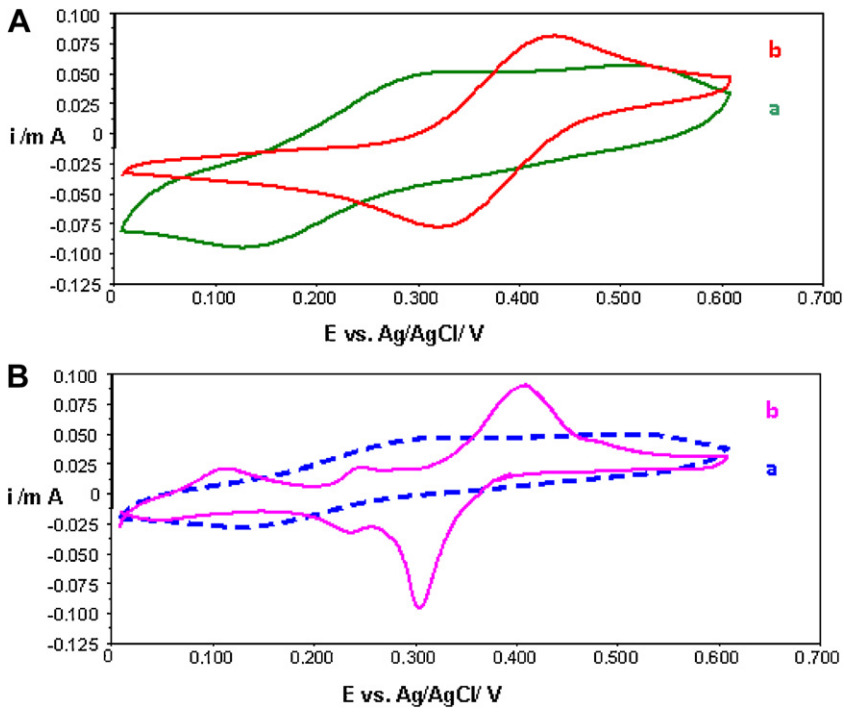

Fig. 4. (A) Cyclic voltammograms (CV) of bare Pt electrode (a) and CHIT/Fe@Au/Pt electrode (b) with 10 mmol L^{-1} $[Fe(CN)_6]^{3-/4-}$ at 0.0 to +0.6 V with a scan rate of 50 mV s^{-1}. (B) Cyclic voltammograms (CV) of modified electrode (a) without and (b) with substrate at 0.0 to +0.6 V with a scan rate of 50 mV s^{-1}.

3.6. Application

The present biosensor was used to estimate erythrocytes GSH levels in healthy person. The mean value of erythrocytes GSH was found to be 2.8 mmol L^{-1} ($n = 10$), which is in normal established range (1–3 mmol L^{-1}).

3.7. Stability and reusability

The biosensor was stored at 4 °C, when not in use. To determine the biosensor storage stability, the amperometric measurements were carried out periodically every fifth day for 4 months. The enzyme electrode lost only 50% of its initial activity after 150 uses

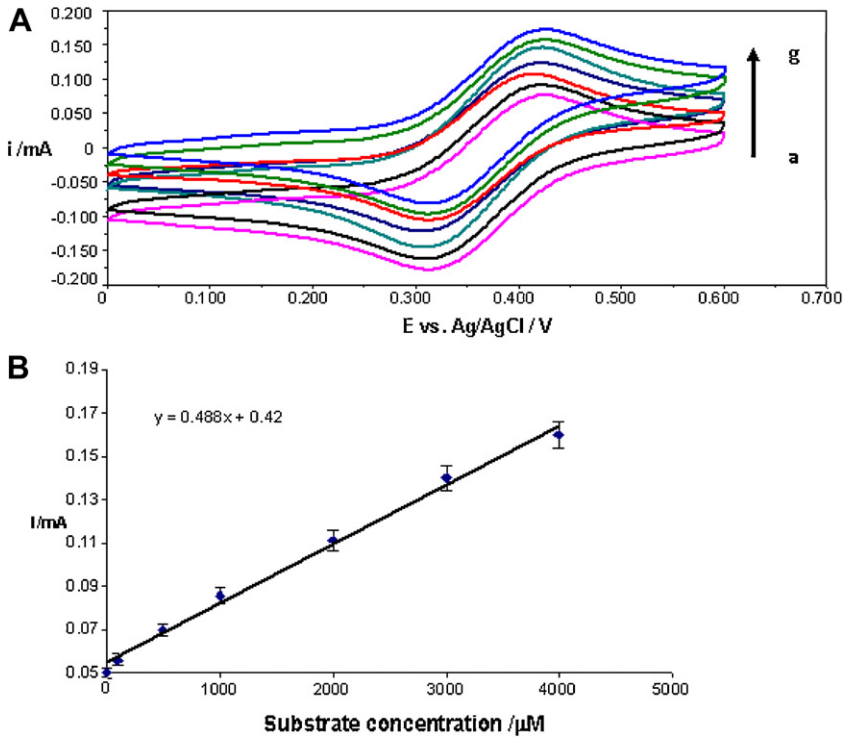

Fig. 5. (A) Cyclic voltammogram of GSHOx/CHIT/Fe@Au modified Pt electrode obtained from 0.0 to +0.6 V in the presence of different concentration of substrate (a) 5.0 μmol L^{-1}, (b) 100 μmol L^{-1}, (c) 500 μmol L^{-1}, (d) 1000 μmol L^{-1}, (e) 2000 μmol L^{-1}, (f) 3000 μmol L^{-1} and (g) 4000 μmol L^{-1} Scan rate of 50 mV s^{-1}.
(B) Standard curve of substrate concentration (Substrate concentration/μM) vs. current (I/mA).

Table 3
A comparison of present GSH biosensor with earlier reported amperometric biosensors.

Matrix/method	Enzyme	Response time	Detection limit (μM)	Linearity	Stability (months)	Reference
Clark-type oxygen electrode/DO metric biosensor	Glutathione oxidase	2 min	5.0	5×10^{-6}–5×10^{-3} M	2	[45]
Pyrolytic graphite-electrode/Amperometric biosensor	Glutathione peroxidase	8 s	ND	1.9×10^{-5}–1.4×10^{-4} M	2	[46]
Teflon membrane/Amperometric inhibition biosensor	Ascorbate oxidase	25 min	0.1	0.1–2 μM	2	[47]
Gold nanoparticle modified Silicon nanowires/Amperometric biosensor	Non-enzymatic	ND	0.33	ND	ND	[20]
Gold coated magnetic nanoparticles modified Pt electrode	Glutathione oxidase	4 s	0.1	5.0–4000 μM	4	Present work

ND: not detected.

during its storage over a period of 4 months, which is better than earlier reports 3 months [44] and 2 months [45–47].

4. Conclusions

GSHOx were covalently immobilized on Pt electrode via amide bond between chitosan and glutaraldehyde. This GSHOx/CHIT/Fe@Au modified Pt electrode reveal improved performance in terms of response time (4 s), linear range (5.0–4000 μmol L^{-1}), sensitivity (0.48 mA/μmol L^{-1}), reusability (more than 150 times) and stability (4 months). The efforts are being made to attest the efficacy of the GSHOx/CHIT/Fe@Au modified Pt electrode using blood samples. The present study showed that GSHOx/CHIT/Fe@Au modified Pt electrode was a very good candidate for the construction of highly sensitive GSH biosensor. The fabricated enzyme electrode exhibited fast amperometric response and high sensitivity for GSH.

References

[1] A. Meister, in: D. Dolphin, R. Poulson, O. Avramovic (Eds.), Glutathione: Chemical, Biochemical and Medical Aspects, Part A, Wiley-Interscience Publication, New York, 1989, pp. 367–434, Chapter 11.
[2] T. Ohkuwa, Y. Sata, M. Naoi, Journal of Chromatography B 705 (1998) 23–28.
[3] J.R. Dunbar, A.J. Delucia, L.R. Bryant, Research Communications in Chemical Pathology and Pharmacology 34 (1981) 485–492.
[4] A. Meister, M.E. Anderson, Annual Review of Biochemistry 52 (1983) 711–760.
[5] E. Obrador, J. Carretero, A. Ortega, I. Medina, V. Rodilla, J.A. Pellicer, J.M. Strela, Hepatology 35 (2002) 74–81.
[6] P.K. Sudeep, S.T.S. Joseph, K.G. Thomas, Journal of the American Chemical Society 127 (2005) 6516–6517.
[7] W. Zhang, F. Wan, W. Zhu, H. Xu, X. Ye, R. Cheng, L.T. Jin, Journal of Chromatography B 818 (2005) 227–232.
[8] N.S. Lawrence, R.P. Deo, J. Wang, Talanta 63 (2004) 443–449.
[9] H. Wang, S.C. Liang, Z.M. Zhang, H.S. Zhang, Analytica Chimica Acta 512 (2004) 281–287.
[10] C.W.I. Owens, R.V. Belcher, Biochemical Journal 94 (1965) 705–711.
[11] I. Rahman, A. Kode, S.K. Biswas, Nature Protocols 1 (2007) 3159–3165.
[12] H.Y. Han, Z.K. He, Y.E. Zeng, Microchimica Acta 155 (2006) 431–434.
[13] B. Ates, B.C. Ercal, K. Manda, L. Abrahama, N. Ercal, Biomedical Chromatography 23 (2009) 119–123.
[14] K.J. Huang, C.H. Han, Y.Y. Wu, C.Q. Han, D.J. Niu, Z.W. Wu, Y.P. Xue, Canadian Journal of Chemistry 89 (2011) 517–523.
[15] J. Lakritz, C.G. Plopper, A.R. Buckpitt, Analytical Biochemistry 247 (1997) 63–68.
[16] J.H.S. Cepeda, T.H.H. Chen, L.H. Fuchigami, Plant and Cell Physiology 32 (1991) 1179–1185.
[17] A.P.F. Turner, Advanced Materials Letters 2 (2011) 82–83.
[18] N.C. Smith, M. Dunnett, P.C. Mills, Journal of Chromatography B 673 (1995) 35–41.
[19] T. Inoue, J.R. Kirchhoff, Analytical Chemistry 72 (2000) 5755–5760.
[20] K. Yang, H. Wang, K. Zou, X. Zhang, Nanotechnology 17 (2006) S276–S279.
[21] S. Kim, J. Kim, H.R. Park, M.K. Kim, C. Yoohoon, W.S. Yeo, Bulletin of the Korean Chemical Society 30 (2009) 2574–2576.
[22] S. Chawla, C.S. Pundir, Biosensors and Bioelectronics 26 (2011) 3438–3443.
[23] S. Kalia, B.S. Kaith, in: Ashutosh Tiwari (Ed.), Degradation of Natural Fibers and Polymer Composites, Polysaccharides: Development Properties and Applications, Nova Science Publishers, Inc., NY, USA, 2010.
[24] E. Bucio, H. Iván Meléndez-Ortiz, T. Isoshima, J. Macossay, Recent Developments in Bio- Nanocomposites for Biomedical Applications, NOVA Science Publishers, Inc., New York, USA, 2011, pp. 207–231, Chapter 12, ISBN 978-1-61761-008-0.
[25] E. Antunes, C. Litwinski, T. Nyokong, Intelligent Nanomaterials, John Wiley & Sons, 2012, pp. 347–324,Chapter 9, ISBN-13: 978-0-470-93879-9.
[26] A.P. Mishra, A. Tiwari, R.K. Jain, Advanced Materials Letters 3 (2012) 213–219.
[27] H. Fang, C.Y. Ma, T.L. Wan, M. Zhang, W.H. Shi, Journal of Physical Chemistry C 111 (2007) 1065–1070.
[28] C.T. Chen, Y.C. Chen, Analytical Chemistry 77 (2005) 5912–5919.
[29] J. Lin, W. Zhou, A. Kumbhar, J. Wiemann, J. Fang, E.E. Carpenter, C.J. O'Connor, Journal of Solid State Chemistry 159 (2001) 26–31.
[30] L.M. Demers, C.A. Mirkin, R.C. Mucic, R.A. Reynolds, R.L. Leitsinger, G.A. Viswanadham, Analytical Chemistry 72 (2000) 5535–5541.
[31] D.K. Kim, M., Mikhaylova, M., Toprak, Y., Zhang, B., Bjelke, J., Kehr, M. Muhammed, In situ gold coating of superparamagnetic nanoparticles by microemulsion method, Materials Research Society Symposium Proceedings 704 (2002) W6.28.6.
[32] M. Mikhaylova, D.K. Kim, C.C. Berry, A. Zogorodni, M. Toprak, A.S.G. Curtis, M. Muhammed, Chemistry of Materials 16 (2004) 2344–2354.
[33] V.K. Mourya, N.N. Inamdar, A. Tiwari, Advanced Materials Letters 1 (2010) 11–33.
[34] S. Cao, R. Mishra, S. Pilla, S. Tripathi, M.K. Pandey, G. Shah, A.K. Mishra, M. Prabaharan, S.B. Mishra, J. Xin, R.R. Pandey, W. Wu, A.C. Pandey, A. Tiwari, Carbohydrate Polymers 82 (2010) 189–194.
[35] Ashutosh Tiwari, Sanjay R. Dhakate, International Journal of Biological Macromolecules 44 (2009) 408–412.
[36] A. Tiwari, Journal of Inorganic and Organometallic Polymers and Materials 19 (2009) 361–366.
[37] A. Tiwari, S. Gong, Electroanalysis 20 (2008) 2119–2126.
[38] S.K. Shukla, S.R., Deshpande, S.K., Shukla, A. Tiwari, Fabrication of a tunable glucose biosensor based on zinc oxide/chitosan-graft-poly(vinyl alcohol) core-shell nanocomposite, Talanta (2012), in press.
[39] Y.S. Kang, S. Risbud, J.F. Rabolt, P. Stroever, Chemistry of Materials 8 (1996) 2209–2211.
[40] J. Jeong, T.H. Ha, B.H. Chung, Analytica Chimica Acta 569 (2006) 203–209.
[41] K.R. Brown, D.G. Walter, M.J. Natan, Chemistry of Materials 12 (2000) 306–313.
[42] T.T.H. Pham, C. Cao, S.J. Sim, Journal of Magnetism and Magnetic Materials 320 (2008) 2049–2055.
[43] S.J. Cho, S.M. Kauzlarich, J. Olamit, K. Liu, F. Grandjean, L. Rebbouh, G. Long, Applied Physics 95 (2004) 6804–6806.
[44] J. Narang, N. Chauhan, P. Jain, C.S. Pundir, International Journal of Biological Macromolecules 50 (2012) 672–678.
[45] D. Compagnone, G. Federici, L. Scarciglia, G. Palleschi, Biosensors and Bioelectronics 8 (1993) 257–263.
[46] L. Rover, L.T. Kubota, N.F. Hoehr, Clinica Chimica Acta 308 (2001) 55–67.
[47] M.K. Sezgintürk, E. Dinçkaya, Biosensors and Bioelectronics 19 (2004) 835–841.